2nd International Congress on 3D Materials Science
Edited by: Dominique Bernard, Jean-Yves Buffière, Tresa Pollock, Henning Friis Poulsen, Anthony Rollett, and Michael Uchic
TMS (The Minerals, Metals & Materials Society), 2014

ATOMIC SCALE AND 3D CHARACTERIZATION OF THE HETEROGENEOUSLY FORMED S (Al_2CuMg) PRECIPITATES AT DISLOCATIONS IN Al-Cu-Mg ALLOY

Zongqiang Feng[1,2], Yanqing Yang[1], Yanxia Chen[1]

[1] Shaanxi Materials Analysis and Research Centre, Northwestern Polytechnical University, Xi'an 710072, China
[2] College of Materials Science and Engineering, Chongqing University, Chongqing 400044, China

Keywords: Aluminum alloy, Precipitation, Dislocations, HRTEM, Electron tomography

Abstract

The variant distribution and three-dimensional (3D) configurations of the heterogeneously formed S (Al_2CuMg) precipitates at dislocations were studied by means of high resolution transmission electron microscopy (HRTEM) and high angle annular dark field scanning transmission electron microscopy (HAADF-STEM) tomography. The preferred S variant pair along dislocation was proved to be S1 & S4 or its counterparts, and the inherent characteristic of the crystal structure of the S phase, i.e. the symmetry of pentagonal subunit, was considered to be the fundamental factor determining the preference of variant pair. The obtained 3D reconstructions of the S precipitates formed at helical dislocations can clearly reveal both the morphology of individual S precipitates and the overall configuration of the S precipitates nucleated at these dislocations.

Introduction

Precipitation in Al-Cu-Mg alloys during artificial ageing can usually take place in either homogeneous or heterogeneous manner. In the case of homogeneous precipitation, the main strengthening phase S (Al_2CuMg) precipitates with needle/rod-like shapes uniformly nucleate in the Al matrix and mainly grows along its $[100]_S$ direction [1]. The orientation relationship (OR) between S precipitate and Al matrix is $[100]_S//[100]_{Al}$, $(001)_S//(012)_{Al}$, which has 12 equivalent variants and four of them, S1~S4, can be seen edge-on in $[100]_{Al}$ direction (Fig. 1) [1,3]. In the case of heterogeneous precipitation, the S precipitates can form at some intrinsic defects such as dislocations, grain boundaries as well as dispersoid/Al interfaces [4]. Specifically, the heterogeneous precipitation of S precipitates at dislocation shows many novel crystallographic and morphological features, hence attracts increasing research concern. By using conventional transmission electron microscopy (TEM), previous researchers have revealed the precipitation process, variant distribution and strengthening effect of S precipitates at dislocations [1,3-7]. To date, however, some major issues, such as the selection criterion for the favorable S variant pair at dislocation, and the spatial distribution characteristics of S precipitates along different morphologies of dislocations, are not yet fully

understood.

In this study, we applied high resolution transmission electron microscopy (HRTEM) and high angle annular dark field scanning transmission electron microscopy (HAADF-STEM) tomography to achieve atomic scale and three-dimensional (3D) characterization of the variant distribution of the heterogeneously formed S precipitates along dislocations, with an attempt to establish the selection rule for favorable variant pair from the crystallographic perspective.

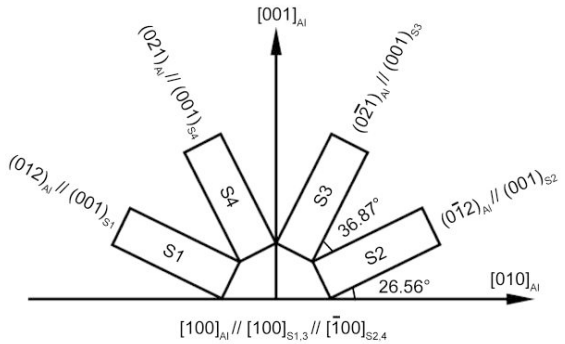

Fig. 1. Schematic illustration of four S variants observed from $[100]_{Al}//[100]_{S1,3}//[\bar{1}00]_{S2,4}$ direction (edge-on).

Experimental

An Al-4.2Cu-1.5Mg-0.6Mn-0.5Fe-0.5Si (wt%) alloy was solution-treated at 495℃ for 45 min, water quenched and then aged at 195℃ for 9h. Two states of the alloy, before and after ageing treatment, were focused on in the present research. Samples for TEM observation were prepared using twin-jet electropolishing in a 30% nitric acid and 70% methanol solution below -25℃ at 15V.

TEM observations were performed on a 300kV field emission TEM, Tecnai F30 G^2, equipped with a fully automated STEM tomography system. A single-tilt holder (Fischione model 2020) and the Xplore 3D software were employed to acquire several tilt series of HAADF-STEM images focusing on the S precipitates at dislocations from -70° to +70°, with an increment of 2° at low angle range (<50°) and of 1° at high angle range (>50°). The tomography data was aligned and reconstructed using Inspect 3D software. The 3D visualization was finally performed using AMIRA 5.2 software.

Results

Fig. 2a shows the microstructure of Al-Cu-Mg alloy after rapid quenching in water from solution temperature, which is characterized by uniformly distributed rod-like T ($Al_{20}Cu_2Mn_3$) dispersoids. Besides, lots of dislocations, especially helical dislocations, can be observed throughout the Al matrix. With further artificial ageing at 195℃ for 9h, high density of needle-like S precipitates aligning along $[001]_{Al}$ and $[010]_{Al}$ directions can be detected in Al matrix, and the helical dislocation lines seem much wider and clearer than their before-ageing state (Fig. 2b), indicating that the heterogeneous precipitation of the S phase has occurred along these dislocations.

Fig. 3 shows a representative HRTEM image of S precipitates at a helical dislocation

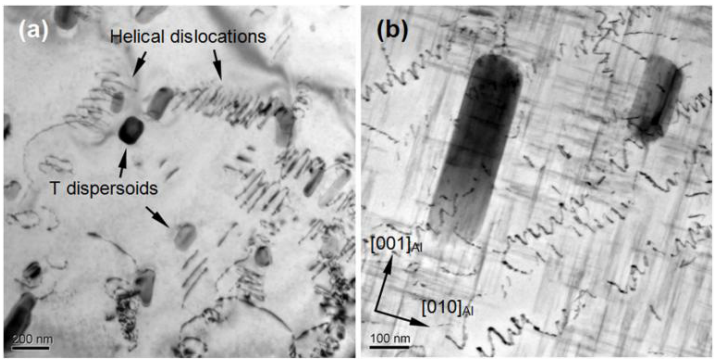

Fig. 2. TEM images showing the microstructure of Al-Cu-Mg alloy (a) before and (b) after artificial ageing at 195℃ for 9h.

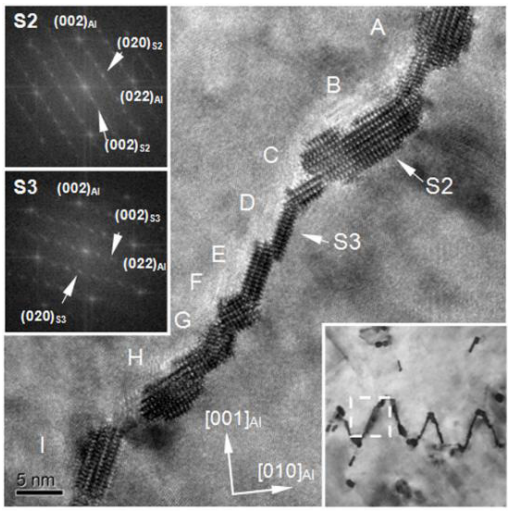

Fig. 3. HRTEM image corresponding to the rectangular region in the bottom-right inset, showing the distribution of S precipitates along a helical dislocation segment. S precipitates A, D, E, G and I belong to variant S3, while B, C, F and H belong to variant S2.

segment, corresponding to that within the rectangular region of the bottom-right inset. The S precipitates A~I, with different cross-sectional shapes but a common $[100]_S$ growth direction, arrange side by side along the original dislocation line. As indicated in the corresponding fast Fourier transformation (FFT) patterns, these precipitates belong to variant S2 or S3, and the only variant pair is S2 & S3.

To further reveal the spatial distribution characteristics from a 3D perspective, HAADF-STEM tomography was performed on several precipitate helices, both perfect and imperfect, to reveal the 3D configurations of the S precipitates along helical dislocations. In the tilt series of HAADF-STEM images of a perfect 'precipitate helix', we can see that the 'precipitate helix' seems like a bandolier-like wavy folded ribbon, in which the S precipitates line up parallel and side by side along the original helical dislocation line (Fig. 4a and 4b). Despite of a little extra diffraction contrast in some HAADF-STEM images, the wavy precipitate bandolier folds can still be seen remarkably in the corresponding 3D reconstruction. Nonetheless, the individual S precipitates can not be clearly distinguished (Fig. 4c), probably due to the poor contrast of such precipitate with a thickness of a few nanometers especially at high tilt angles. In the tilt series of HAADF-STEM images of an imperfect 'precipitate helix' (Fig. 4d and 4e) and the corresponding 3D reconstruction (Fig. 4f), separate S phase precipitates can be observed at several sites as labeled by arrows. All

these S precipitates show needle-like morphology and have a common elongation direction. Based on HRTEM observation (Fig. 3) and HAADF-STEM tomography, a schematic drawing showing the distribution of needle-/lath-like S precipitates along helical dislocations is illustrated in Fig. 4g.

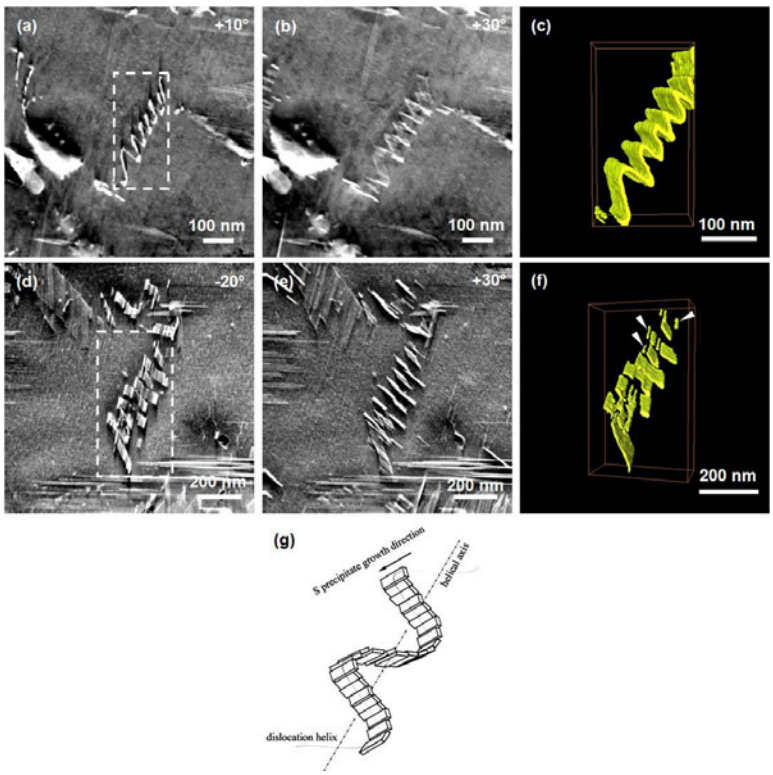

Fig. 4. Two tilt series of HAADF-STEM images and the corresponding 3D tomographic reconstructions showing the distribution of S precipitates along helical dislocations. (a,b) and (d,e) are representative HAADF-STEM images from the respective tilt series while (c) and (f) are tomographic reconstructions of the full dataset corresponding to the rectangular regions in (a) and (d). Note that the needle-like S precipitates all point in a $<100>_{Al}$ direction with the individual precipitates labeled by arrows. (g) Schematic illustration showing the distribution of S precipitates along helical dislocations.

Discussion

As representatively shown in Fig. 3, S precipitates along a dislocation line always have a common $[100]_S$ growth direction, and the only favorable variant pair is S2 & S3 or their counterpart S1 & S4, with relevant $(001)_S$ planes having a relative angular separation of 36.87° (Fig. 1). Such phenomenon has been proved by many previous investigations [2-4]. To elucidate why the variant pair of S2 & S3 or their counterpart S1 & S4 is the most favorable for S precipitates along dislocations, former researchers tried to relate the intrinsic characteristics of dislocation (line direction, Burgers vector) with those of precipitates (habit plane, maximum misfit vector) [2,3,8]. However, these selection criteria of variant pairs are still in dispute, mainly because neither the morphology or the Burger vector of the original dislocation on which the S precipitate forms can be observed or determined any more after long time elevated ageing and precipitate nucleation. In fact, the variant pair of S1 & S4 or their counterpart S2 & S3 is prefered not only for S precipitates along dislocations, but for

those at grain boundaries and phase interfaces [4]. Accordingly, the selection criterion for favorable variant pair of S precipitates needs to be revisited with consideration of the nucleation resistance and the inherent characteristic of the crystal structure of the S phase.

Generally, to form an energetically favorable variant pair, two conditions should be satisfied as much as possible: (i) each S variant keeps the classic OR and coherent interfaces with the Al matrix, i.e. $(001)_S//\{021\}_{Al}$, and (ii) S variants in the same pair share an interface with the lowest energy to utmostly reduce the nucleation resistance. Fig. 5 schematically illustrates the spatial distribution and crystal structure of three possible S variant pairs in $[100]_{Al}//[100]_{S1,3}//[\bar{1}00]_{S2,4}$ direction (edge-on view) according to the classic OR between S precipitate and Al matrix. Every S variant contains a 2×2 unit cell of the S phase. From the perspective of crystallography, when looking down the $[100]_S$ direction, several pentagonal subunits can be observed within the unit cell of the S phase (black line pentagons). The adjoining pentagons share the same edge and are centrosymmetrical about the center of the sharing edge. To our knowledge, regular pentagon always goes together with the 36° angle. The twinning operation to a regular pentagon is actually equivalent to a 36° rotation. As shown in Fig. 5a, for S1 and S4 (equivalent to S2 and S3) with classic OR with Al matrix, theoretically we can calculate that the angle between $(001)_{S1}$ and $(001)_{S4}$ is 36.87°, which is very close to the rotation angle required to form a twin of a regular pentagon. In this sense, S1 and S4 can be considered as twins. With a slight rotation (0.87°), the adjoining pentagonal subunits can share the same edge and form a coherent twin interface, which can significantly reduce the nucleation energy of the correlative S variants. However, for variant pair of S1 and S3 (equivalent to S2 and S4), to form such a coherent twin interface, at least a 18° rotation is required but the coherent relationship of $(001)_S//\{021\}_{Al}$ will be destroyed (Fig. 5b), indicating the nucleation resistance increases for S precipitates. The variant combination of S1 and S2 (equivalent to S3 and S4) is not common since a much larger rotation angle (54°) is necessary to make the adjacent pentagons edge-sharing and form a coherent twin interface (Fig. 5c), thus the nucleation resistance to form this variant pair of S precipitates will be even larger. In a word, the variant pair of S1 and S4 or their counterpart is energetically favorable, and the inherent characteristic of the crystal structure of the S phase, i.e. the symmetry of the

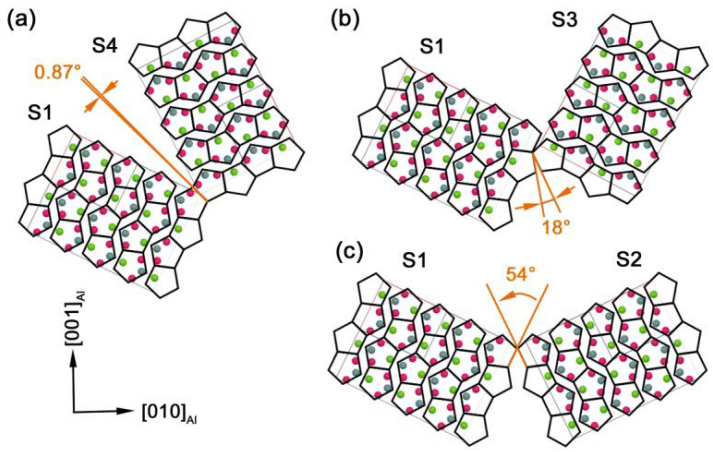

Fig. 5. Schematic illustration showing the spatial distribution and crystal structure of three possible S variant pairs in $[100]_{Al}//[100]_{S1,3}//[\bar{1}00]_{S2,4}$ direction. Every S variant contains a 2×2 unit cell of the S phase, and the black line pentagon outlines the subunits in the S phase structure. (a) S1 & S4; (b) S1 & S3; (c) S1 & S2.

pentagonal subunit, may be the fundamental factor determining the preference of variant pair.

With the help of HAADF-STEM tomography, we successfully obtained 3D reconstructions of the S precipitates along helical dislocations, in which both the wavy feature of these S precipitate groups and the needle-like morphology of an individual S precipitate can be clearly observed (Fig. 4c and 4f). This, together with the HRTEM observations, fully reveals the spatial distribution of the S variants along helical dislocation lines. HAADF-STEM tomography was proved to be a promising technique for studies of nanoscale precipitates, or their assembly, with complex morphology or configuration in metallic alloys.

Conclusions

HRTEM and HAADF-STEM tomography was applied to systematically investigate the variant distribution and 3D configurations of the heterogeneously formed S precipitates at dislocations in an Al-Cu-Mg alloy. The favorable S variant pair along dislocations was revealed and the underlying selection rule was discussed from the crystallographic perspective. In the 3D reconstruction of the S precipitates formed at helical dislocations, both the morphology of individual S precipitates and the overall configuration of the S precipitates nucleated at these dislocations can be clearly observed, which provided new evidence for variant distribution of S precipitates along dislocations.

Acknowledgements

Financial support from Excellent Doctorate Foundation of Northwestern Polytechnical University and the 111 Project (B08040) of China is gratefully acknowledged.

References

1. S.C. Wang and M.J. Starink, “Precipitates and intermetallic phases in precipitation hardening Al-Cu-Mg- Li alloy,” *International Materials Reviews*, 50 (2005),193-215.
2. R.N. Wilson and P.G. Partridge, “The nucleation and growth of S' precipitates in an aluminium-2.5% copper-1.2% magnesium alloy,” *Acta Metallurgica*, 13 (1965), 1321-1327.
3. Z.Q. Feng et al., “Variant selection and the strengthening effect of S precipitates at dislocations in Al-Cu-Mg alloy,” *Acta Materialia*, 59 (2011), 2412-2422.
4. Z.Q. Feng et al., “HRTEM and HAADF-STEM tomography investigation of the heterogeneously formed S (Al_2CuMg) precipitates in Al-Cu-Mg alloy,” *Philosophical Magazine*, 93 (2013), 1843-1858.
5. P. Ratchev et al., “Precipitation hardening of an Al-4.2wt% Mg-0.6wt% Cu alloy,” *Acta Materialia*, 46 (1998), 3523-3533.
6. A. Tolley, R. Ferragut and A. Somoza, “Microstructural characterisation of a commercial Al-Cu-Mg alloy combining transmission electron microscopy and positron annihilation spectroscop,” *Philosophical Magazine*, 89 (2009), 1095-1110.
7. Z.Q. Feng et al., “Precipitation process along dislocations in Al-Cu-Mg alloy during artificial aging,” *Materials Science and Engineering A*, 528 (2010), 706-714.
8. A. Kelly and R.B. Nicholson, “Precipitation hardening,” *Progress in Materials Science*, 10 (1963), 151-391.